

Actin-based motility of vaccinia virus mimics receptor tyrosine kinase signalling

Friedrich Frischknecht, Violaine Moreau, Sabine Röttger, Stefania Gonfloni*, Inge Reckmann, Giulio Superti-Furga* & Michael Way

Cell and * Developmental Biology Programmes, European Molecular Biology Laboratory, Meyerhofstrasse 1, 69117 Heidelberg, Germany

Studies of the actin-based motility of the intracellular pathogens *Listeria monocytogenes* and *Shigella flexneri* have provided important insight into the events occurring at the leading edges of motile cells^{1–5}. Like the bacteria *Listeria* and *Shigella*, vaccinia virus, a relative of the causative agent of smallpox, uses actin-based motility to spread between cells⁶. In contrast to *Listeria* or *Shigella*, the actin-based motility of vaccinia is dependent on an unknown phosphotyrosine protein, but the underlying mechanism remains obscure⁷. Here we show that phosphorylation of tyrosine 112 in the viral protein A36R by Src-family kinases is essential for the actin-based motility of vaccinia. Tyrosine phosphorylation of A36R results in a direct interaction with the adaptor protein Nck⁸ and the recruitment of the Ena/VASP family member N-WASP⁹ to the site of actin assembly. We also show that Nck and N-WASP are essential for the actin-based motility of vaccinia virus. We suggest that vaccinia virus spreads by mimicking the signalling pathways that are normally involved in actin polymerization at the plasma membrane.

We began our investigation into the mechanism of actin-based motility of vaccinia virus by identifying the phosphotyrosine protein observed at the site of actin assembly⁷. Western-blot analysis reveals that three prominent proteins, pTyr200, pTyr80/85 and pTyr50, consistently become tyrosine phosphorylated during vaccinia infection (Fig. 1). Western-blot analysis and immunoprecipitation experiments identified pTyr80/85 as the actin-binding protein cortactin¹⁰ (data not shown), which is known to be enriched in the cell cortex and becomes phosphorylated by c-Src when *Shigella* enters the cell¹¹. To determine whether tyrosine phos-

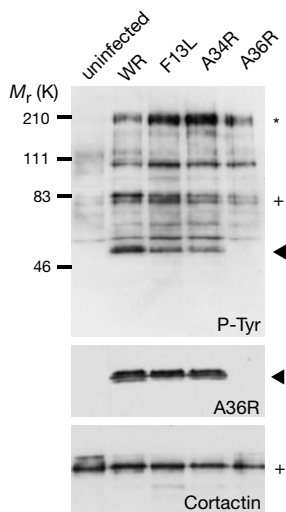


Figure 1 Vaccinia A36R protein is tyrosine phosphorylated. Top, western-blot analysis of phosphotyrosine proteins during vaccinia infection reveals that three proteins, pTyr200 (asterisk), pTyr80/85 (cross) and pTyr50 (arrowhead) consistently become tyrosine phosphorylated, although pTyr50 (arrowhead) is absent in Δ A36R infections. Bottom, the same blot probed with A36R and cortactin antibodies. Virus strains are indicated.

phorylation of pTyr200, pTyr80/85 and pTyr50 was dependent on actin tail formation, we examined the phosphorylation pattern of cells infected with the recombinant viral strains Δ A34R, Δ A36R and Δ F13L, which do not induce actin tails at 8 hours post-infection^{12,13}. We found that pTyr50 was absent in cells infected with a recombinant virus lacking A36R (Fig. 1). Western-blot analysis of two-dimensional gels and immunoprecipitation experiments showed that pTyr50 and A36R are the same protein (data not shown). The vaccinia A36R protein is a type Ib integral membrane protein with a cytoplasmic domain of about 200 amino-acid residues¹³ that plays

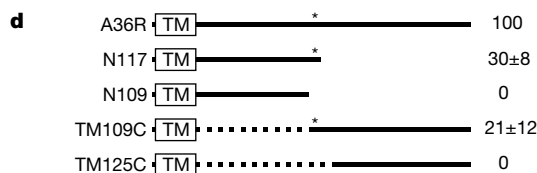
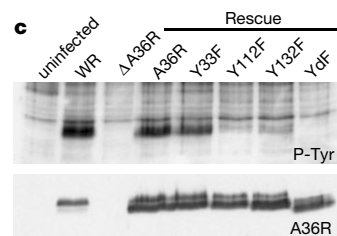
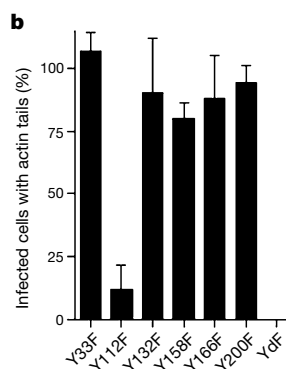
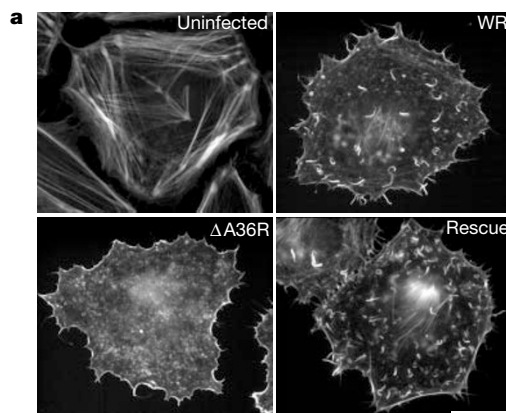


Figure 2 Tyrosine phosphorylation of A36R is essential for vaccinia actin tail formation. **a**, Immunofluorescence analysis reveals that ectopic expression of A36R in the Δ A36R background rescues actin tail formation. Scalebar, 20 μ m. **b**, Quantification of actin tail formation by all six A36R tyrosine-to-phenylalanine mutants reveals that only Y112 is required for efficient actin tail formation. However, only the A36R–YdF double mutant (Y112F and Y132F combined) eliminates all actin tail formation. **c**, Top, western-blot analysis of ectopically expressed A36R point mutants reveals that Δ A36R-infected cells expressing Y112F or Y132F have a weaker pTyr50 signal than cells infected with WR, or with Δ A36R expressing wild-type A36R or Y33F. Y158F, Y166F and Y200F mutants are phosphorylated to a similar extent as A36R or Y33F (data not shown). No pTyr50 signal is detectable in Δ A36R-infected cells expressing the YdF double mutant. Bottom, the same blot reprobed with anti-A36R antibody. YdF migrates slightly faster than the other A36R proteins, consistent with an absence of tyrosine phosphorylation. **d**, Diagram of A36R and the deletion mutants N109, N117, TM109C and TM125C (see Methods for nomenclature). The box at the N terminus shows the predicted transmembrane domain (TM). Asterisk indicates Y112; dotted line indicates the region of A36R that is deleted in TM109C and TM125C; numbers on the right show the rescue efficiencies of actin tail formation.

an essential but undefined role in the actin-based motility of vaccinia^{12,14}.

To study the role of A36R phosphorylation in vaccinia actin-based motility, we tested whether ectopic expression of the wild-type A36R protein in Δ A36R infected cells would rescue actin tail formation. Ectopic expression of A36R resulted in both tyrosine phosphorylation of the protein and efficient rescue of actin tail formation ($111 \pm 36\%$) (Fig. 2a, c). Expression of point mutants of the six individual tyrosine residues in the A36R cytoplasmic domain showed that only a change of tyrosine 112 to phenylalanine (A36R mutant Y112F) resulted in a dramatic reduction of actin tails (Fig. 2b). However, western-blot analysis revealed that mutation of either tyrosine 112 or tyrosine 132 reduced A36R phosphorylation, indicating that both of these residues are phosphorylated (Fig. 2c). As A36R–Y112F still rescues actin tail formation, albeit at low levels, we produced the double point mutant, YdF, in which both residues 112 and 132 were changed to phenylalanine. Although expression of A36R–YdF was similar to the other point mutants, we found no evidence for either tyrosine phosphorylation of the protein or rescue of actin tail formation (Fig. 2b, c). Lack of rescue was not due to mistargeting, as A36R–YdF localized to the intracellular enveloped form of vaccinia virus, which is responsible for actin tail formation⁶ (data not shown). In parallel with studies using A36R point mutants, we examined the ability of several A36R deletion constructs to rescue actin tail formation (Fig. 2d). The only requirement for actin tail formation was the presence of tyrosine 112, which represents a good Src-family kinase phosphorylation site¹⁵. Vaccinia infection also induces phosphorylation of cortactin, a well known Src substrate¹⁰, so we tested whether this family of kinases phosphorylates A36R. We found that the Src-family kinase-inhibitor PP1 (ref. 16) reduced tyrosine phosphorylation of both A36R and cortactin, as well as reducing actin tail formation (Fig. 3a; and data not shown). However, PP1 did not affect viral assembly or A36R localization (data not shown). In addition, expression of c-Src kinase ‘dead open’ mutants 527 Kin⁻ and KP Kin⁻ reduced tyrosine phosphorylation of A36R and actin tail formation (Fig. 3a, b; and data not shown). When expressed at low levels, 527 Kin⁻ and KP Kin⁻ were observed at the site of vaccinia actin tail formation, which is consistent with their dominant-negative activity when overexpressed (Fig. 3c).

Our observations that vaccinia actin tail formation is dependent on Src-family kinases and tyrosine phosphorylation is reminiscent

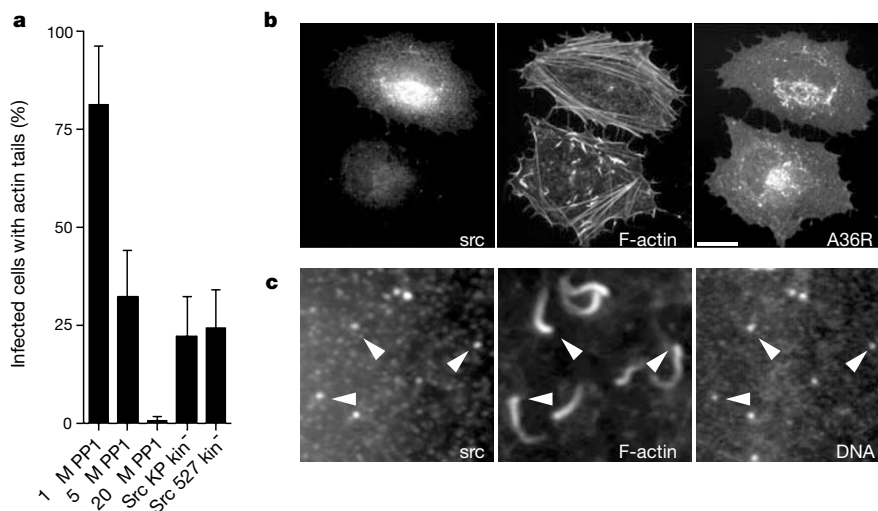


Figure 3 Src-family kinases mediate actin tail formation of vaccinia virus. **a**, The Src-family kinase inhibitor PP1 inhibits actin tail formation in a dose-dependent manner. Overexpression of dead open c-Src mutants also reduces the efficiency of actin tail formation. **b**, Immunofluorescence analysis of the effects of overexpressing dead open

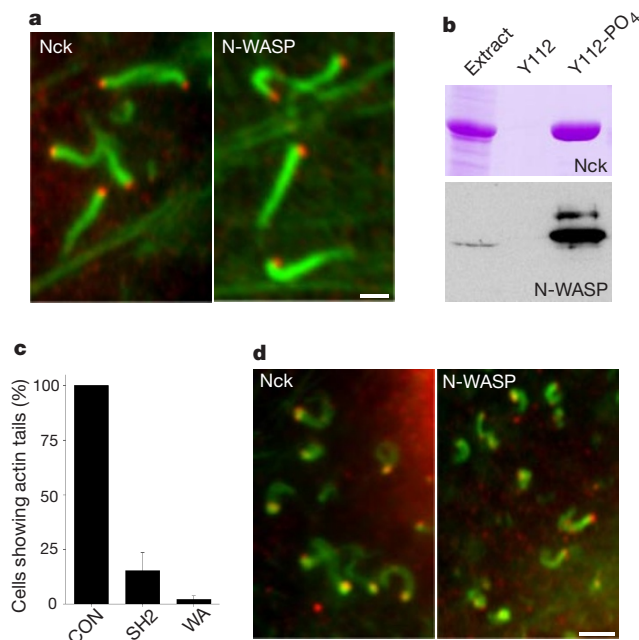


Figure 4 Nck and N-WASP are essential for vaccinia actin tail formation.

a, Immunofluorescence images showing that Nck and N-WASP (red) are recruited to vaccinia virus particles that have induced actin tails (green). Scale bar, 2 μ m. **b**, Top, Coomassie-stained gel showing that the peptide A36R105-116 containing phosphorylated tyrosine 112 interacts directly with Nck, as it retains the protein from soluble *Escherichia coli* extract. Y112 and Y112-PO₄ represent the unphosphorylated and phosphorylated versions of the A36R105-116 peptide, respectively. Bottom, western blot showing that the Nck-A36R105-116 complex recruits N-WASP from extracts prepared from infected cells. The resin sample represents five times more material than the extract sample, demonstrating there is no recruitment of N-WASP by the unphosphorylated A36R105-116 peptide. **c**, Overexpression of the Nck-SH2 domain (SH2) or an N-WASP construct lacking the WA domain (Δ WA) inhibits actin tail formation in WR-infected cells. CON, control cells infected with WR but not transfected. **d**, Immunofluorescence images showing that Nck and N-WASP (red) are recruited to clathrin-coated vesicles that can nucleate actin tails (green) in uninfected cells. Scale bar, 2 μ m.

c-Src mutants on vaccinia actin tail formation. Two infected cells, one transfected (top) and one untransfected (bottom), are shown. Scale bar, 20 μ m. **c**, Closer examination of infected cells expressing low levels of dead open c-Src reveals that the protein is recruited to viral particles that have induced actin tails (arrowheads).

of signal-transduction pathways involved in the control of actin polymerization at the plasma membrane. This analogy is strengthened by the localization of the adaptor protein Nck⁸ at the site of vaccinia actin tail formation (Fig. 4a). Nck recruitment was dependent on both A36R and its phosphorylation, as it was absent in Δ A36R infections, with or without ectopic expression of A36R–YdF (data not shown). *In vitro* binding assays using peptides corresponding to residues 105–116 of A36R demonstrate that recruitment of Nck to the virus occurs through the direct interaction with A36R and is dependent on phosphorylation of tyrosine 112 (Fig. 4b). Furthermore, overexpression of the Nck SH2 domain resulted in a dramatic reduction of actin tail formation (Fig. 4c). The involvement of Nck raises the question whether its downstream partner WASP^{8,17,18} is also required for vaccinia actin tail formation. We found that N-WASP⁹, a member of the Ena/VASP family, is recruited to the virus (Fig. 4a). N-WASP was also efficiently recruited from cell extracts by the Nck–A36R-phosphorylated peptide complex (Fig. 4b). As observed with the Nck SH2 domain, overexpression of a dominant-negative construct, N-WASP– Δ WA¹⁹, inhibits actin tail formation (Fig. 4c). The requirement of N-WASP, which is known to stimulate the actin-nucleating activity of the Arp2/3 complex^{20,21}, seems to provide the final link to achieve vaccinia actin tail formation. Nck and N-WASP, together with the Arp2/3 complex, are also observed on clathrin-coated vesicles that can nucleate little actin tails⁷ (Fig. 4), indicating that this complex of proteins plays an important role in initiating actin polymerization in the cell.

Vaccinia virus therefore achieves actin-based motility by mimicking the receptor tyrosine kinase signalling pathways that control actin polymerization at the plasma membrane. The sequence conservation between vaccinia A36R and its homologue A39R in variola virus, the causative agent of smallpox, indicates that variola virus also used actin-based motility to spread between cells. This Src-family kinase-dependent signalling pathway may also account for other cellular effects induced by vaccinia infection, including induction of cell motility, loss of contact inhibition and changes in cell adhesion, all of which are reminiscent of a transformed phenotype^{22,23}. We suggest that vaccinia virus provides an excellent model system in which to study Src-family kinase and the signalling pathways that affect actin polymerization, adhesion and cell motility. □

Methods

Western-blot and immunofluorescence analysis

Western reserve and recombinant vaccinia strains that lack the genes A34R, A36R or F13L are referred to as WR, Δ A34R, Δ A36R and Δ F13L¹². HeLa cells were infected and processed for western-blot or immunofluorescence analysis, and images were acquired as described^{7,13}. Intracellular enveloped virions were labelled with A33R or A36R antibodies¹³, and tyrosine-phosphorylated proteins were detected with the 4G10 monoclonal antibody (Upstate Biotechnology). Src was detected by using anti-Src 327 mouse monoclonal antibody²⁴. Antibodies against cortactin and Nck were obtained from Upstate Biotechnology, Transduction Laboratories and Santa Cruz Biotechnology. Rhodamine- and Alexa 488-phalloidin and PP1 were obtained from Molecular Probes and Alexis Corporation, respectively.

Construction of pEL A36R expression vectors

A36R expression was placed under the control of the synthetic vaccinia virus early/late promoter (E/L)²⁵ by polymerase chain reaction (PCR) using the primers pELA36RFor 5′-CCGCCGCTCGAGAAAATTGAAATTTTATTTTATTTTGGAAATATAA-TAAGCTCGAGATCTACCATGATGCTGGTACCTCTTATC-3′ and A36RH3Rev 5′-GGCAAGCTTATCACCAATGATACGACCGATGATCTAT-3′. The resulting PCR product was cloned into the *Xho*I–*Hind*III sites of *Not*I-deficient pBluescript SKII to generate the pELA36R construct. Tyrosine-to-phenylalanine point mutations of A36R were engineered by ‘round the world’ PCR²⁶ using pELA36R as a template. The pELA36R–YdF construct was engineered in the same way using A36R–Y112F as the template. The deletion mutants N109 and N117 were generated by introducing a stop codon after residue 109 and 117, respectively, and are named according to the remaining sequence, that is, amino-terminal to their final carboxy-terminal residue (Fig. 2d). We took advantage of a unique SnaB1 site, which immediately follows the transmembrane (TM) domain of A36R (residues 1–32) to generate internal deletions by PCR. Internal deletions TM109C and TM125C are defined by the presence of the transmembrane domain followed by the first residue of the cytoplasmic domain of A36R (109 or 125) extending to the C terminus (Fig. 2d).

pEL dominant-negative expression constructs

*Eco*RI–*Bam*HI inserts containing the *c*-Src mutants 527 Kin[−] and KP Kin[−] were cloned into the *Eco*RI–*Bgl*II sites of the pELA36R vector backbone. The 527 and KP of the K295M catalytically dead (Kin[−]) *c*-Src represent mutations of Y527F and K249G/P250E²⁴, respectively. These proteins represent ‘dead open’ conformations of *c*-Src which are able to bind cellular targets but are catalytically inactive. EGFP was amplified by PCR from the pEGFP-N1 expression vector (Clontech) and cloned into the *Bgl*III–*Xho*I sites of pEL immediately downstream of the viral promoter. The DNA coding residues 1–397 of rat N-WASP⁹ were then amplified by PCR and cloned into the *Not*I–*Eco*RI sites of the pELGFP vector to generate pELGFP N-WASP– Δ WA, which lacks the WH2 and acidic domains of the protein¹⁹. The DNA corresponding to the SH2 domain, residues 275–373, of human Nck1 and the full-length protein were amplified by PCR from a HeLa cDNA library and cloned in an identical fashion to N-WASP– Δ WA into pELGFP. The fidelity of all pEL constructs was confirmed by sequencing.

Expression and quantification of actin tail rescue or inhibition

pEL constructs were transfected into HeLa cells 4 hours post-infection with either WR or Δ A36R viral strains and processed for immunofluorescence or western-blot analysis 4 hours later. Similarly, PP1 was added to cells either before infection or up to 4 hours post-infection. Rescue of actin tail formation or inhibition efficiencies were determined from over 200 infected cells in 4 independent experiments based on criteria described previously⁷. All data were normalized to WR or A36R rescue experiments where appropriate, and error bars indicate standard deviation of the mean.

Protein expression and *in vitro* binding

Human Nck1 was cloned from pELGFP into the vector pMW172, expressed in BL21(DE3), and the soluble fraction prepared as described²⁷. The tyrosine-phosphorylated and unphosphorylated versions of the peptide CCGAPSTEHYDVSAGST, corresponding to residues 105–116 of A36R, were coupled by the N-terminal cysteine residue to Sulfolink resin (Pierce). The BL21(DE3) soluble fraction containing Nck1 was incubated with peptide resin in the presence of 1 mM vanadate at room temperature for 30 min and washed 5 times with phosphate-buffered saline containing 100 mM NaCl, 0.1% Tween and 1 mM vanadate. The washed resin was then incubated with cell extracts prepared as described¹³. Samples were removed for SDS–PAGE and western-blot analysis to assess Nck1 and N-WASP binding.

Received 23 June; accepted 19 August 1999.

1. Dramsi, S. & Cossart, P. Intracellular pathogens and the actin cytoskeleton. *Annu. Rev. Cell Dev. Biol.* **14**, 137–166 (1998).
2. Finlay, B. B. & Cossart, P. Exploitation of mammalian host cell functions by bacterial pathogens. *Science* **276**, 718–725 (1997).
3. Welch, M. D., Iwamoto, A. & Mitchison, T. J. Actin polymerization is induced by Arp2/3 protein complex at the surface of *Listeria monocytogenes*. *Nature* **385**, 265–269 (1997).
4. Welch, M. D., Rosenblatt, J., Skole, J., Portnoy, D. A. & Mitchison, T. J. Interaction of human Arp2/3 complex and the *Listeria monocytogenes* ActA protein in actin filament nucleation. *Science* **281**, 105–108 (1998).
5. Mullins, D. R., Heuser, J. A. & Pollard, T. D. The interaction of Arp2/3 complex with actin: nucleation, high affinity pointed end capping, and formation of branching networks of filaments. *Proc. Natl. Acad. Sci. USA* **95**, 6181–6186 (1998).
6. Cudmore, S., Cossart, P., Griffiths, G. & Way, M. Actin-based motility of vaccinia virus. *Nature* **378**, 636–638 (1995).
7. Frischknecht, F. *et al.* Tyrosine phosphorylation is required for actin based motility of vaccinia but not *Listeria* or *Shigella*. *Curr. Biol.* **9**, 89–92 (1999).
8. McCarty, J. H. The Nck SH2/SH3 adaptor protein: a regulator of multiple intracellular signal transduction events. *BioEssays* **20**, 913–921 (1998).
9. Miki, H., Minura, K. & Takenawa, T. N-WASP, a novel actin-depolymerizing protein, regulates the cortical cytoskeletal rearrangement in a PIP2-dependent manner downstream of tyrosine kinases. *EMBO J.* **15**, 5326–5335 (1996).
10. Wu, H. & Parsons, J. T. Cortactin, an 80/85-kilodalton pp60src substrate, is a filamentous actin-binding protein enriched in the cell cortex. *J. Cell Biol.* **120**, 1417–1426 (1993).
11. Dehio, C., Prevost, M. C. & Sansonetti, P. J. Invasion of epithelial cells by *Shigella flexneri* induces tyrosine phosphorylation of cortactin by a pp60src-mediated signalling pathway. *EMBO J.* **14**, 2471–2482 (1995).
12. Sanderson, C. M., Frischknecht, F., Way, M., Hollinshead, M. & Smith, G. L. Roles of vaccinia virus EEV-specific proteins in intracellular actin tail formation and low pH-induced cell-cell fusion. *J. Gen. Virol.* **79**, 1415–1425 (1998).
13. Röttger, S., Frischknecht, F., Reckmann, I., Smith, G. L. & Way, M. Interactions between vaccinia virus IEV membrane proteins and their roles in IEV assembly and actin tail formation. *J. Virol.* **73**, 2863–2875 (1999).
14. Wolffe, E. J., Weisberg, A. S. & Moss, B. Role for the vaccinia virus A36R outer envelope protein in the formation of virus-tipped actin-containing microvilli and cell-to-cell virus spread. *Virology* **25**, 20–26 (1998).
15. Songyang, Z. & Cantley, L. C. Recognition and specificity in protein tyrosine kinase-mediated signalling. *Trends Biochem. Sci.* **20**, 470–475 (1995).
16. Hanke, J. H. *et al.* Discovery of a novel, potent, and src family selective tyrosine kinase inhibitor. *J. Biol. Chem.* **271**, 695–701 (1996).
17. Rivero-Lezcano, O. M. & Marcilla, A., Sameshima, J. H. & Robbins, K. C. Wiskott-Aldrich syndrome protein physically associates with Nck through Src3 homology domains. *Mol. Cell Biol.* **15**, 5725–5731 (1995).
18. Snapper, S. B. & Rosen, F. S. The Wiskott-Aldrich syndrome protein (WASP): roles in signalling and cytoskeletal organization. *Annu. Rev. Immunol.* **17**, 905–929 (1999).
19. Machesky, L. M. & Insall, R. H. Scar1 and the related Wiskott-Aldrich syndrome protein WASP regulate the actin cytoskeleton through the Arp2/3 complex. *Curr. Biol.* **8**, 1347–1356 (1998).

20. Machesky, L. M. *et al.* Scar, a WASP-related protein, activates dendritic nucleation of actin filaments by the Arp2/3 complex. *Proc. Natl Acad. Sci. USA* **96**, 3739–3744 (1999).
21. Rohatgi, R. *et al.* The interaction between N-WASP and the Arp2/3 complex links Cdc42-dependent signals to actin assembly. *Cell* **97**, 221–231 (1999).
22. Sanderson, C. M., Way, M. & Smith, G. L. Virus-induced cell motility. *J. Virol.* **72**, 1235–1243 (1998).
23. Sanderson, C. M. & Smith, G. L. Vaccinia virus induces calcium-independent cell-matrix adhesion during the motile phase of infection. *J. Virol.* **72**, 9924–9933 (1998).
24. Gonfloni, S. *et al.* The role of the linker between the SH2 domain and catalytic domain in the regulation and function of Src. *EMBO J.* **16**, 7261–7271 (1997).
25. Chakrabarti, S., Sisler, J. R. & Moss, B. Compact, synthetic, vaccinia virus early/late promoter for protein expression. *Biotechniques* **23**, 1094–1097 (1997).
26. Hemsley, A., Arnheim, N., Toney, M. D., Cortopassi, G. & Galas, D. J. A simple method for site-directed mutagenesis using the polymerase chain reaction. *Nucleic Acids Res.* **17**, 6545–6551 (1989).
27. Way, M., Pope, B. & Weeds, A. G. Evidence for functional homology in the F-actin binding domain of gelsolin and alpha-actinin: implications for the requirements of severing and capping. *J. Cell Biol.* **119**, 835–842 (1992).

Acknowledgements

We are grateful to H. Miki for N-WASP cDNA and N-WASP antibody. We thank G. Smith and R. Blasco for providing recombinant vaccinia strains; J. White, C. Blaumüller, A. Desai and A. Plobidou for reading the manuscript; T. Harder for encouraging us to try PP1; and S. Guth for the 'round the world' PCR method. S.G. was supported by a fellowship from the Boncompagni-Ludovisi Foundation.

Correspondence and requests for materials should be addressed to M.W. (e-mail: way@embl-heidelberg.de).

Asynchronous replication of imprinted genes is established in the gametes and maintained during development

Itamar Simon*, Toyooki Tenzen†‡, Benjamin E. Reubinoff‡, Dahlia Hillman‡, John R. McCarrey§ & Howard Cedar*

* Department of Cellular Biochemistry, Hebrew University, Jerusalem 91120, Israel

† Department of Evolutionary Genetics, National Institute of Genetics, Mishima, Shizuoka-ken 411-8540, Japan

‡ Department of Obstetrics and Gynecology, Hadassah Ein-Kerem University Hospital, Jerusalem 91120, Israel

§ Department of Genetics, Southwest Foundation for Biomedical Research, San Antonio, Texas 78228, USA

Genomic imprinting is characterized by allele-specific expression of multiple genes within large chromosomal domains¹ that undergo DNA replication asynchronously during S phase^{2,3}. Here we show, using both fluorescence *in situ* hybridization analysis and S-phase fractionation techniques, that differential replication timing is associated with imprinted genes in a variety of cell types, and is already present in the pre-implantation embryo soon after fertilization. This pattern is erased before meiosis in the germ line, and parent-specific replication timing is then reset in late gametogenesis in both the male and female. Thus, asynchronous replication timing is established in the gametes and maintained throughout development, indicating that it may function as a primary epigenetic marker for distinguishing between the parental alleles.

Fluorescence *in situ* hybridization (FISH) analysis on interphase nuclei can be used to assay the replication properties of individual alleles in nonsynchronously growing cells⁴. For most gene regions, one observes either two single or two double hybridization dots per nucleus, indicating that both alleles replicate at about the same time in S phase. In contrast, FISH analysis of mono-allelically expressed sequences, such as imprinted genes² or olfactory receptor genes⁵,

reveals a large number of nuclei in which one allele has already replicated while the other has not, thus indicating asynchronous replication. Interestingly, this pattern is regional and is found in a variety of cell types independent of expression^{2,3}, suggesting that it is also preserved during development.

Imprinted gene regions have a parent-of-origin specific replication pattern^{2,3}. In contrast, the olfactory receptor gene loci replicate in a random manner; in some cells the paternal allele replicates early, whereas in others the maternal allele replicates early⁵. This latter pattern is similar to that seen with the X chromosome in female cells.

Although the FISH approach provides a good measure of replication timing and a sensitive way to detect allelic asynchrony^{2,3,6,7}, we wanted to show directly that imprinted genes do replicate with an asynchronous pattern, as determined by quantitative polymerase chain reaction (PCR) analysis of pulse-labelled BrdU DNA⁸ from S-phase-sorted cell fractions⁹. As shown in Fig. 1a, the human *Igf2* gene in EBV-transformed lymphocytes replicates in a broad peak covering the middle of S phase. Use of a restriction-site polymorphism to distinguish between the two alleles, however, shows that one chromosomal copy clearly replicates before the other despite considerable overlap (Fig. 1a). In a similar experiment, we characterized the replication properties of the mouse *Igf2r* gene using an Abelson-transformed pre-B-cell subclone from Spretus/Musculus F₁ mice (Fig. 1b). Here, the replication pattern of each allele is clearly separable. As the pedigree of these cells is known, this system also allowed us to prove that it is the paternal Spretus allele that replicates early².

Unlike the FISH methodology, which detects the sharp endpoint of replication, the resolving power of cell-cycle fractionation techniques is low, probably because DNA replication may not initiate at exactly the same time within every individual cell, and because there is considerable overlap in the fluorescence-sorted S-phase fractions. This might help explain why in studies using similar techniques, but based on fewer S-phase fractions, the *Igf2/H19* locus did not appear to replicate asynchronously^{10,11}. In fact, a careful visual re-examination of the raw data from one of these studies¹⁰ reveals allelic differences very similar to those seen in our own PCR analyses. Thus, these results indicate that FISH analysis provides a reliable and accurate method for detecting asynchronous replication, and has the advantage that it can be used on small cell populations *in vivo*.

To understand the functional relationship between genomic

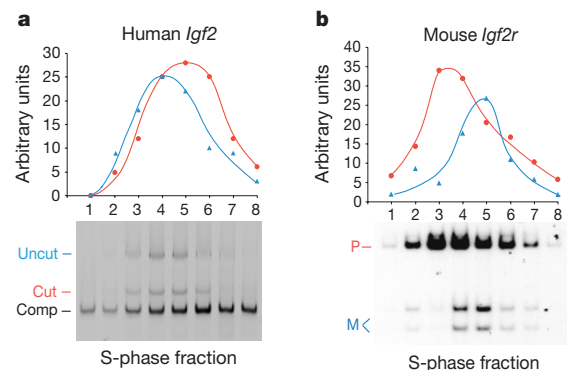


Figure 1 Detection of asynchronous timing by S-phase fractionation. Replication timing was analysed by S-phase fractionation of BrdU-labelled DNA (see Methods) using restriction enzymes to distinguish between the paternal (P) and maternal (M) alleles of *Igf2* in EBV-transformed human lymphoblasts (a) and *Igf2r* in mouse Abelson-transformed pre-B cells (b). When these same B cells were analysed by FISH, we detected 44% single/single (SS), 35% single/double (SD) and 21% double/double (DD) signals. After subtracting normal background (~18% SD), the difference between the two alleles is roughly 15%, or ~1–1.5 h, a time difference similar to that seen in the Figure. Circles, uncut alleles; triangles, cut alleles. Comp, competitor DNA product.